

# Hyperconjugative Stabilization in Alkyl Carbocations: Direct Estimate of the $\beta$ -Effect of Group-14 Elements

Israel Fernández and Gernot Frenking\*

Fachbereich Chemie, Philipps-Universität Marburg, Hans-Meerwein Strasse, 35043 Marburg, Germany

Received: May 15, 2007; In Final Form: May 26, 2007

DFT calculations at the BP86/TZ2P level have been carried out for the primary, secondary, and tertiary carbenium ions  $[\text{H}_2\text{C}-\text{CH}(\text{EH}_3)_2]^+$  (**1a-e**),  $[\text{HC}\{\text{CH}(\text{EH}_3)_2\}_2]^+$ , (**2a-e**), and  $[\text{C}\{\text{CH}(\text{EH}_3)_2\}_3]^+$  (**3a-e**) for E = C, Si, Ge, Sn, Pb. The nature of the interaction between the carbenium center  $\text{H}_{2-n}\text{C}^+$  and the substituents  $\{\text{CH}(\text{EH}_3)_2\}_m$  has been investigated with an energy decomposition analysis (EDA) aiming at estimating the strength of the  $\pi$  hyperconjugation which electronically stabilizes the carbenium ions. The results of the EDA show that the calculated  $\Delta E_\pi$  values can be used as a measure for the strength of hyperconjugation in carbenium ions arising from the interactions of saturated groups possessing  $\pi$  orbitals. The theoretical data suggest that the ability of  $\sigma$  C–E bonds to stabilize positive charges by hyperconjugation follow the order  $\text{C} \ll \text{Si} < \text{Ge} < \text{Sn} < \text{Pb}$ . Hyperconjugation of C–Si bonds is much stronger than hyperconjugation of C–C bonds while the further rising from silicon to lead is smaller and has about the same step size for each element. The strength of the hyperconjugation in primary, secondary, and tertiary alkyl carbenium ions does not increase linearly with the number of hyperconjugating groups; the incremental stabilization becomes smaller from primary to secondary to tertiary cations. The effect of hyperconjugation is reflected in the shortening of the C–C bond distances and in the lengthening of the C–E bonds, which exhibits a highly linear relationship between the calculated C–C and C–E distances in carbocations **1–3** and the hyperconjugation estimated by the  $\Delta E_\pi$  values.

## Introduction

Carbocations are arguably the most important reactive intermediates in organic chemistry.<sup>1</sup> Meerwein suggested in 1922 for the first time that positively charged alkyl cations might be involved in a chemical reaction.<sup>2</sup> He recognized that the rearrangement reactions of camphene hydrochloride showed similarities with the behavior of triarylhalomethanes, which could be understood if ionization takes place during the reaction. Meerwein's proposal was a breakthrough in physical organic chemistry<sup>3</sup> because later research revealed that carbocations are the key for understanding not only rearrangement reactions but for many other organic processes like substitution and elimination reactions.<sup>1</sup> Carbocations may be distinguished into five-coordinated species (carbonium ions) and three-coordinated species (carbenium ions). A particular class of carbenium ions which is termed nonclassical ions has hydrogen atoms or other groups in a bridging position to the electron deficient positively charged carbon atom. Nonclassical cations have been the topic of intensive theoretical and experimental research.<sup>4</sup>

The parent carbenium ion  $\text{CH}_3^+$  is not stable in a condensed phase. Substitution of hydrogen by substituents which are capable of donating electronic charge into the formally empty  $p(\pi)$  AO stabilizes the cations which may eventually become isolated and characterized with spectroscopic methods. Groups which carry lone-pair electrons such as  $\text{NR}_2$ , OR, or halides are particularly suitable for stabilizing carbenium ions.<sup>1</sup> Another possibility for yielding stable carbocations is through conjugation with a  $\pi$ -electron systems, yielding conjugated species such as

allyl or benzyl cations which are notably stable species. Saturated groups are generally less suitable for stabilizing carbenium ions because hyperconjugation (Figure 1) is less efficient than conjugation. Recent theoretical studies by us and others have shown, however, that stabilization due to hyperconjugation is not negligible and that it may significantly contribute to the structure and stability of molecules.<sup>5,6</sup>

Hyperconjugative stabilization in a carbenium ion  $\text{CR}_3^+$  involves the donation of electronic charge from a substituent R, which has no multiple bonds into the formally empty  $p(\pi)$  orbital of the carbenium carbon atom. Figure 1a depicts a situation where the hyperconjugative stabilization in an alkyl carbenium ion consists of genuine  $\pi$  interactions such as conjugative interactions because the cation possesses an appropriate mirror plane. The difference between hyperconjugation and conjugation is that in the latter interaction the substituent has a multiple bond consisting of  $\sigma$  and  $\pi$  bonding and that the charge donation comes from the  $\pi$  component. The charge donation from an electronically saturated substituent comes from an orbital which has local  $\sigma$  symmetry. This is the reason that hyperconjugation is often referred to as donation from an occupied  $\sigma$  orbital into an empty  $\pi$  orbital. Figure 1b depicts a situation where the methyl group is rotated about the C–C bond by  $90^\circ$ . The hyperconjugation now takes place between an occupied orbital of the  $\text{CH}_3$  group and the vacant p orbital of C(+) atom, which in the strictest sense have  $\sigma$  symmetry because they are symmetric with respect to the mirror plane of that conformation. However, these orbitals have  $\pi$  character because the sign of the orbital changes in the local  $\text{H}_2\text{C}(+)\text{--C}$  plane which is not a mirror plane of the ethyl cation conformation depicted in Figure 1b. The resulting orbital is therefore

\* To whom correspondence should be addressed. Phone: +49(0)-6421-282 5563. Fax: +49(0)6421-282 5566. E-mail: frenking@chemie.uni-marburg.de.

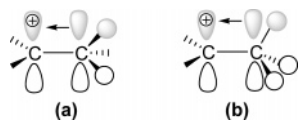


**Figure 1.** Schematic representation of hyperconjugation in an alkyl carbenium cation. (a) Hyperconjugative charge donation from an occupied  $\pi$  orbital of the alkyl substituent. (b) Hyperconjugative charge donation from an occupied  $\sigma$  orbital (pseudo- $\pi$  orbital) of the alkyl substituent.

said to possess pseudo- $\pi$ -symmetry.<sup>7</sup> In this paper we only investigate systems which correspond to the situation which is sketched in Figure 1a.

It is well-known that alkyl-substituted carbenium ions  $\text{CR}_3^+$  exhibit the stability order tertiary > secondary > primary >  $\text{CH}_3^+$ . Until very recently, the only aliphatic cations which could become structurally characterized by X-ray analysis were tertiary carbocations like the adamantyl cation<sup>8</sup> and the *tert*-butyl cation.<sup>9</sup> Bochman and co-workers now report about the first isolation and X-ray structure determination of a secondary alkyl carbenium ion.<sup>10</sup> The remarkably stable crystal compound  $[\text{HC}\{\text{CH}(\text{SiMe}_3)(\text{SnMe}_3)\}_2]^+\text{Zr}_2\text{Cl}_9^-$  melts at 109 °C while the analogous species with  $\text{Hf}_2\text{Cl}_9^-$  as counterion melts at 120 °C. The X-ray structure analysis of the former cation shows that there are no close contacts between the cation and the anion.<sup>10</sup> The authors reported also about DFT calculations of the secondary carbenium ion and related all-silicon model compounds. It was suggested that the stability of the cation comes from hyperconjugation, where the C–Sn bonds which are in a  $\beta$  position should be much more effective than the C–Si bonds. Evidence for the suggestion comes from analysis of the charge distribution, the geometry and from the NMR chemical shifts.<sup>10</sup> The same conclusion was achieved experimentally by Lambert<sup>11</sup> through comparison of the extrusion reaction of  $\text{Me}_3\text{MX}$  from  $\text{Me}_3\text{MCH}_2\text{CH}_2\text{X}$  ( $\text{M} = \text{Si to Sn}$ ;  $\text{X} = \text{nucleofuge}$ ) in solvents of different nucleophilicities and theoretically by Gordon<sup>12</sup> through comparison of the isodesmic reactions of  $\text{H}_3\text{MCH}_2\text{CH}_2^+$  and  $\text{CH}_3^+$ .

The stabilizing  $\beta$ -effect of group-14 elements which is widely employed in synthetic transformations<sup>13</sup> was the topic of extensive experimental and theoretical studies with the goal to elucidate the origin of the stabilization.<sup>14</sup> A pivotal question concerns the strength of the hyperconjugative stabilization which is the driving force of the  $\beta$ -effect. It would be helpful if a direct estimate of the strength of the hyperconjugation could be made based on a well-defined quantum chemical partitioning of the interaction energy which does not need an external reference system. A method which uses only the  $\pi$  orbitals of the interacting fragments in the geometry of the molecule for estimating  $\pi$  interactions is the energy decomposition analysis (EDA).<sup>15</sup> We recently reported that the calculated  $\Delta E_\pi$  values given by the EDA can be used as a probe to estimate the relative contributions of  $\pi$  interactions which come from conjugation between multiple bonds or from hyperconjugation which arise from the interactions of saturated groups possessing  $\pi$  orbitals.<sup>5f,5g,16</sup> We successfully applied this method in order to compare the calculated strength of the  $\pi$  conjugation in meta- and para-substituted benzylic cations and anions with Hammett substituent constants.<sup>16a</sup> The advantage of the EDA calculations for estimating the strength of  $\pi$  interactions was revealed by the excellent correlation between the calculated  $\Delta E_\pi$  values and experimental data such as the <sup>13</sup>C NMR chemical shifts in large  $\pi$  conjugated systems.<sup>16b</sup>

The good performance of the EDA encouraged us to employ the method for a theoretical investigation of the  $\beta$ -effect in

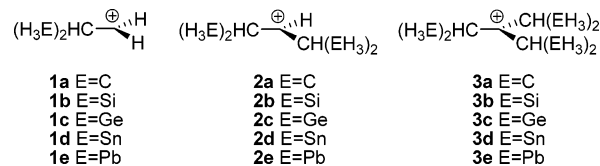


**Figure 2.** Schematic representation of the primary (**1a–e**), secondary (**2a–e**), and tertiary (**3a–e**) alkyl carbenium ions investigated in this work.

primary, secondary and tertiary alkyl carbocations which carry C–E bonds ( $\text{E} = \text{C–Pb}$ ). We calculated the geometries and analyzed the bonding situation in the carbenium ions  $[\text{H}_2\text{C–CH}(\text{EH}_3)_2]^+$  (**1a–e**),  $[\text{HC}\{\text{CH}(\text{EH}_3)_2\}_2]^+$  (**2a–e**), and  $[\text{C}\{\text{CH}(\text{EH}_3)_2\}_3]^+$  (**3a–e**) ( $\text{E} = \text{C–Pb}$ ), which are shown in Figure 2. The calculated data give detailed information about the interatomic interactions in the cations. The theoretical work should be helpful for further experimental work which aims at the synthesis of carbenium ions.

## Methods

The geometries of the molecules have been optimized at the nonlocal DFT level of theory using the exchange functional of Becke<sup>17</sup> in conjunction with the correlation functional of Perdew<sup>18</sup> (BP86). Uncontracted Slater-type orbitals (STOs) were employed as basis functions for the SCF calculations.<sup>19</sup> The basis sets have triple- $\zeta$  quality augmented by two sets of polarization functions, that is, p and d functions for the hydrogen atoms and d and f functions for the other atoms. This level of theory is denoted as BP86/TZ2P. An auxiliary set of s, p, d, f, and g STOs was used to fit the molecular densities and to represent the Coulomb and exchange potentials accurately in each SCF cycle.<sup>20</sup> Scalar relativistic effects have been considered using the zero-order regular approximation (ZORA).<sup>21</sup> The vibrational frequencies of the optimized structures have been calculated in order to investigate the nature of the stationary points. The Hessian matrices of the optimized geometries have in all cases only positive eigenvalues which means that the fully optimized structures reported here are minima on the potential energy surface. The atomic partial charges were calculated by using the Hirshfeld partitioning scheme.<sup>22</sup>

The calculations were carried out with the program package ADF 2003.<sup>23</sup> The interactions were analyzed by means of the energy decomposition analysis (EDA) of ADF,<sup>15</sup> which was developed by Ziegler and Rauk<sup>24</sup> following a similar procedure suggested by Morokuma.<sup>25</sup> EDA has proven to give important information about the nature of the bonding in main-group compounds and transition-metal complexes.<sup>26</sup> The focus of the bonding analysis is the instantaneous interaction energy,  $\Delta E_{\text{int}}$ , of the bond, which is the energy difference between the molecule and the fragments in the electronic reference state and frozen geometry of the compound. The interaction energy can be divided into three main components:

$$\Delta E_{\text{int}} = \Delta E_{\text{elstat}} + \Delta E_{\text{Pauli}} + \Delta E_{\text{orb}} \quad (1)$$

$\Delta E_{\text{elstat}}$  gives the electrostatic interaction energy between the fragments, which are calculated using the frozen electron density distribution of the fragments in the geometry of the molecules. The second term in eq 1,  $\Delta E_{\text{Pauli}}$ , refers to the repulsive interactions between the fragments, which are caused by the fact that two electrons with the same spin cannot occupy the same region in space.  $\Delta E_{\text{Pauli}}$  is calculated by enforcing the Kohn–Sham determinant on the superimposed fragments to obey the Pauli principle by antisymmetrization and renormal-

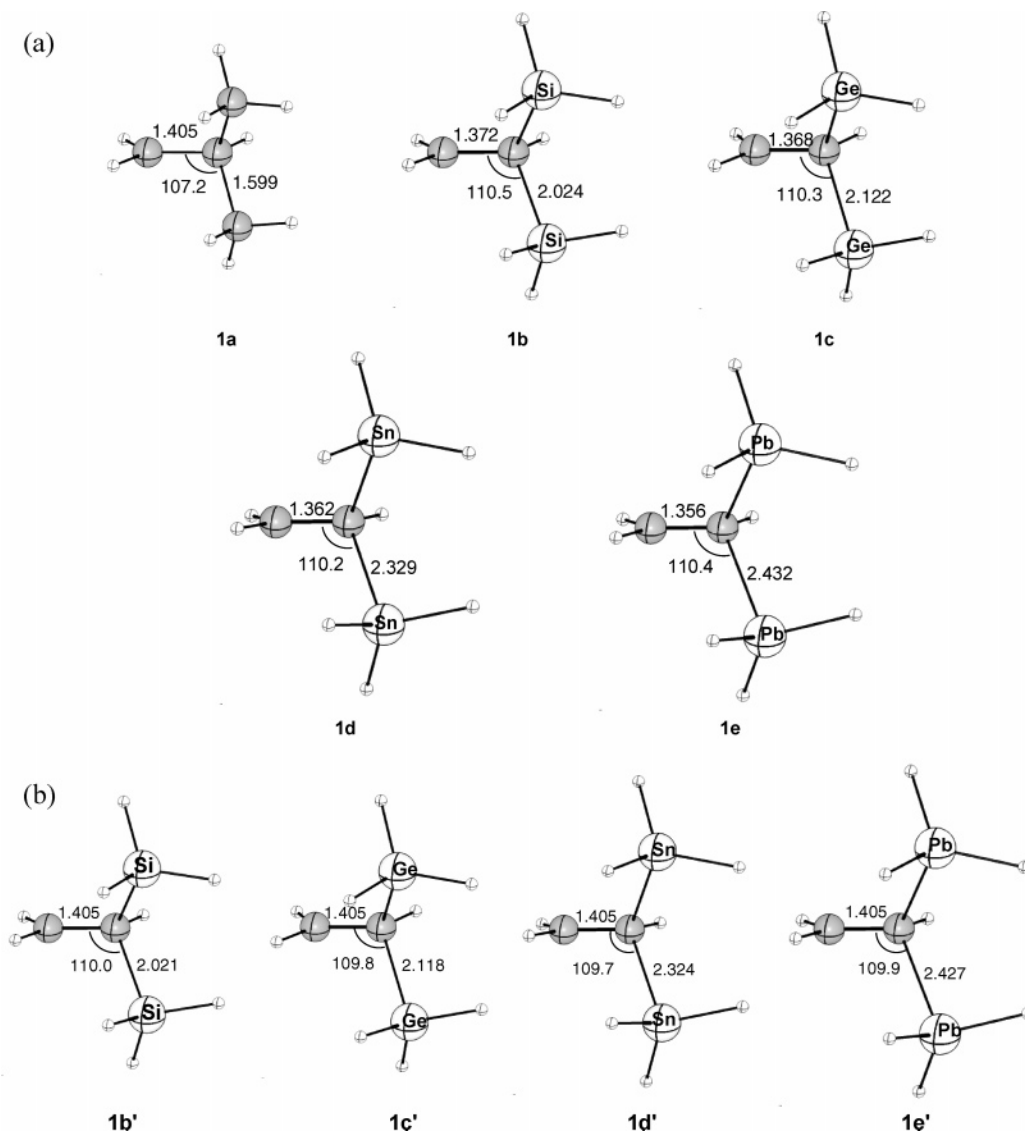


**Figure 3.** (a) Fully optimized geometries at BP86/TZ2P of (a) **1a–e**. (b) Partially optimized geometries at BP86/TZ2P of **1b'–e'** where the C–C distance is kept frozen at the value of **1a** (1.405 Å). Bond distances are given in Å and angles in deg.

ization. The stabilizing orbital interaction term,  $\Delta E_{\text{orb}}$ , is calculated in the final step of the energy partitioning analysis when the Kohn–Sham orbitals relax to their optimal form. This term can be further partitioned into contributions by the orbitals belonging to different irreducible representations of the point group of the interacting system. The interaction energy,  $\Delta E_{\text{int}}$ , can be used to calculate the bond dissociation energy,  $D_e$ , by adding  $\Delta E_{\text{prep}}$ , which is the energy necessary to promote the fragments from their equilibrium geometry to the geometry in the compounds (eq 2). The advantage of using  $\Delta E_{\text{int}}$  instead of  $D_e$  is that the instantaneous electronic interaction of the fragments becomes analyzed which yields a direct estimate of the energy components. Further details of the energy partitioning analysis can be found in the literature:<sup>15</sup>

$$-D_e = \Delta E_{\text{prep}} + \Delta E_{\text{int}} \quad (2)$$

The interacting fragments in the EDA calculations are the open-shell species which come from breaking the  $\sigma$  bond(s) between them. The calculations of the open shell fragments for the EDA can only be carried out in the ADF program using the restricted formalism while for the optimization of the fragments the unrestricted formalism is used. The energy differences

between the restricted and unrestricted calculations were always  $<1$  kcal/mol. The difference is included in the  $\Delta E_{\text{prep}}$  values.

## Results and Discussion

**Primary Carbenium Ions.** We optimized the geometries of the primary cations  $[\text{H}_2\text{C}-\text{CH}(\text{EH}_3)_2]^+$  where  $E = \text{C}-\text{Pb}$  (**1a–e**) using  $C_s$  symmetry constraints. Figure 3 shows the most important bond lengths and angles. The calculated  $\text{H}_2\text{C}-\text{C}$  bond distances which are significantly shorter than a normal C–C single bond systematically decrease from **1a** (1.405 Å) to **1e** (1.356 Å). The shortening suggests that the hyperconjugative stabilization of the C–E bonds increases in the order C–C  $<$  C–Si  $<$  C–Ge  $<$  C–Sn  $<$  C–Pb. Figure 3 shows also the structures of the cations **1b'–e'**, which have been optimized with a frozen C–C distance of **1a** (1.405 Å). The latter calculations were carried out in order to estimate in the EDA study the intrinsic strength of the hyperconjugation of the C–E bonds using identical C–C bond lengths. Note that the C–E distances in **1b'–e'** are only slightly shorter than in **1b–e**.

Table 1 summarizes the EDA results of the carbocations **1a–e** using the fragments  $\text{CH}_2^+$  and  $\text{CH}(\text{EH}_3)_2$  in the respective doublet state where the unpaired electron is in a  $\sigma$  orbital as interacting species which yield the carbon–carbon bond. The

TABLE 1: Results of the Energy Decomposition Analysis for Cations **1a–e** and **1b'–e'** at BP86/TZ2P<sup>a</sup>

$$(\text{H}_3\text{E})_2\text{HC}^{\oplus}\text{H}$$

	<b>1a</b> , E = C	<b>1b</b> , E = Si	<b>1b'</b> , E = Si	<b>1c</b> , E = Ge	<b>1c'</b> , E = Ge	<b>1d</b> , E = Sn	<b>1d'</b> , E = Sn	<b>1e'</b> , E = Pb	<b>1e</b> , E = Pb
symmetry	$C_s$	$C_s$	$C_s$	$C_s$	$C_s$	$C_s$	$C_s$	$C_s$	$C_s$
$\Delta E_{\text{int}}$	-180.0	-213.3	-211.4	-222.6	-220.5	-234.6	-232.2	-244.7	-241.9
$\Delta\Delta E_{\text{int}}^b$	—	-33.3	—	-9.3	—	-12.0	—	-10.1	—
$\Delta E_{\text{Pauli}}$	295.8	305.2	280.0	311.9	282.6	322.1	287.4	334.3	293.8
$\Delta E_{\text{elstat}}^c$	-176.1 (37.0%)	-170.2 (32.8%)	-159.6 (32.5%)	-174.9 (32.7%)	-162.4 (32.3%)	-180.5 (32.4%)	-166.0 (31.9%)	-188.1 (32.5%)	-171.2 (31.9%)
$\Delta E_{\text{orb}}^c$	-299.7 (63.0%)	-348.2 (67.2%)	-331.8 (67.5%)	-359.6 (67.3%)	-340.7 (67.7%)	-376.2 (67.6%)	-353.6 (68.1%)	-390.8 (67.5%)	-364.6 (68.1%)
$\Delta E_{\sigma}^d$	-237.2 (79.2%)	-247.8 (71.2%)	-236.9 (71.4%)	-249.8 (69.5%)	-237.5 (69.7%)	-255.0 (67.8%)	-240.2 (67.9%)	-258.9 (66.2%)	-241.8 (66.3%)
$\Delta E_{\pi}^d$	-62.4 (20.8%)	-100.4 (28.8%)	-94.9 (28.6%)	-109.8 (30.5%)	-103.2 (30.3%)	-121.2 (32.2%)	-113.4 (33.1%)	-131.9 (33.8%)	-122.8 (33.7%)
$\Delta\Delta E_{\pi}^e$	—	-38.0	—	-9.4	—	-11.4	—	-10.7	—
$\Delta E_{\text{prep}}$	22.3	34.0	32.6	33.5	32.2	32.7	31.2	32.9	31.1
$\Delta E (= -D_e)$	-157.7	-179.3	-178.8	-189.1	-188.3	-201.9	-201.0	-211.8	-210.8
$r(\text{C-C})$ (Å)	1.405	1.372	—	1.368	—	1.362	—	1.356	—
$q(\text{C})^f$	0.221	0.113	—	0.082	—	0.047	—	0.021	—
$q(\text{E})^g$	-0.034	0.423	—	0.405	—	0.524	—	0.521	—

<sup>a</sup> Energy values in kcal/mol. Compounds **1b'–e'** have been calculated using the C–C bond length of **1a**. <sup>b</sup> Increase of  $\Delta E_{\text{int}}$  with respect to the preceding molecule. <sup>c</sup> The percentages in parentheses give the contribution to the total attractive  $\Delta E_{\text{elstat}} + \Delta E_{\text{orb}}$ . <sup>d</sup> The percentages in parentheses give the contribution to the orbital interactions  $\Delta E_{\text{orb}}$ . <sup>e</sup> Increase of  $\Delta E_{\pi}$  with respect to the preceding molecule. <sup>f</sup> Atomic partial charge at central carbon atom. <sup>g</sup> Atomic partial charge at atom E.

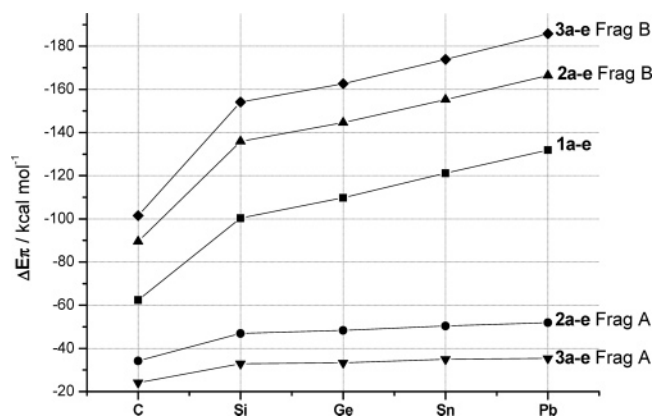


Figure 4. Trend of the calculated strength of  $\pi$  interactions  $\Delta E_{\pi}$  for the elements  $E = \text{C} - \text{Pb}$  in carbocations **1–3**.

strength of the total  $\text{H}_2\text{C}^+ - \text{CH}(\text{EH}_3)_2$  interactions  $\Delta E_{\text{int}}$  increases for E with the order  $\text{C} < \text{Si} < \text{Ge} < \text{Sn} < \text{Pb}$ . The same trend is also found for the calculated bond dissociation energy  $D_e$  although the increase from carbon to silicon is alleviated because of the concomitant increase of the preparation energy for the fragments  $\Delta E_{\text{prep}}$ .

Inspection of the three energy terms which aid to  $\Delta E_{\text{int}}$  show that in all cases, the largest contribution to the C–C attraction comes from the orbital term  $\Delta E_{\text{orb}}$ , which accounts for about two-third of the binding energy while the electrostatic term  $\Delta E_{\text{elstat}}$  adds one-third. The most important information for the present study comes from the breakdown of  $\Delta E_{\text{orb}}$  into  $\sigma$  and  $\pi$  bonding. The data in Table 1 show that there is a systematic increase of the absolute values but also of the percentage contribution of  $\Delta E_{\pi}$  to  $\Delta E_{\text{int}}$ . A graphical display for the trend is shown in Figure 4. It becomes obvious that the increase is particularly strong from C to Si while the further rising from Si to Pb exhibits nearly identical slopes. The increase in the  $\pi$  bonding is given by the  $\Delta\Delta E_{\pi}$  values shown in Table 1. A striking result is the finding that the latter values are very close to the increase in the total interaction energy  $\Delta\Delta E_{\text{int}}$ . Although the  $\pi$ -orbital interactions are only a minor contributor to the

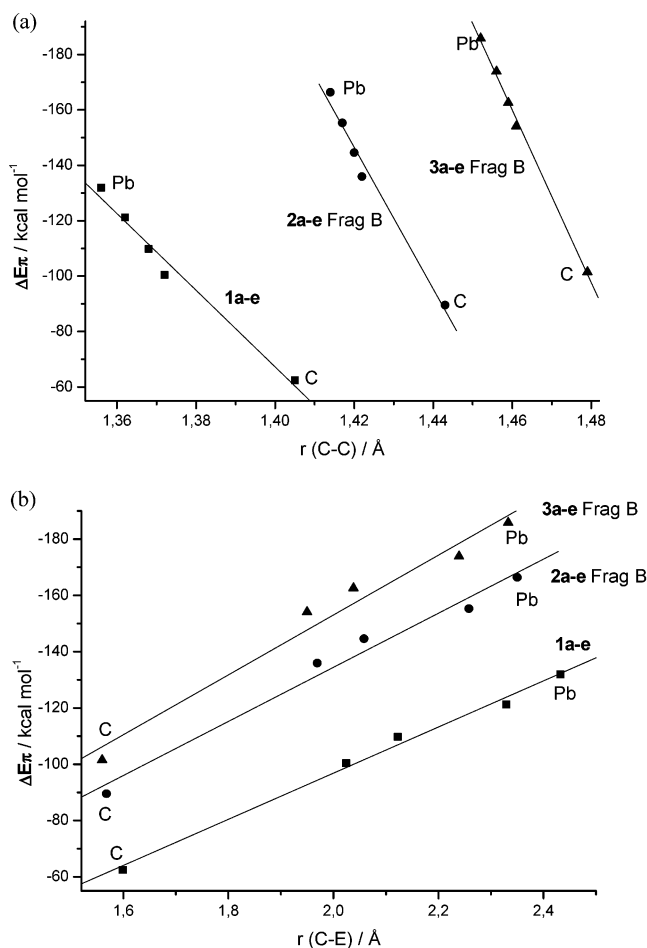
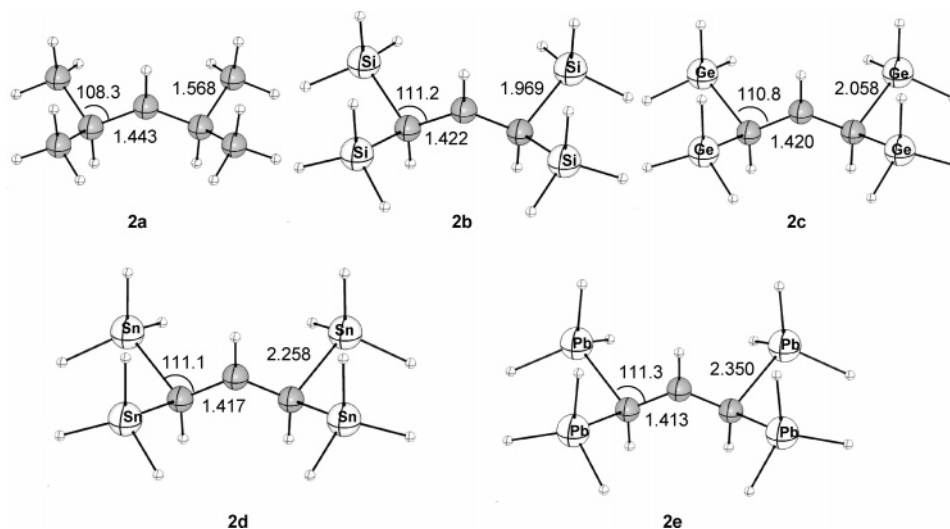


Figure 5. Correlation of the calculated  $\Delta E_{\pi}$  values for carbocations **1–3** with: (a) C–C bond lengths; (b) C–E bond lengths.

total binding they strongly correlate with the overall trend given by  $\Delta E_{\text{int}}$ . This is a very important result because it provides quantitative support for the model where the increase in the C–C binding interactions in the cations  $[\text{H}_2\text{C} - \text{CH}(\text{EH}_3)_2]^+$  is



**Figure 6.** Fully optimized geometries at BP86/TZ2P of **2a–e**. Bond distances are given in Å and angles in deg.

explained with the hyperconjugation of the C–E bonds. The strength of the hyperconjugation is mainly an intrinsic property of the C–E  $\pi$ -orbitals which is only slightly amplified by the concomitant shortening of the H<sub>2</sub>C–C bond lengths. This becomes obvious from the EDA results for the compounds **1b'–e'** given in Table 1 which were optimized with the same C–C bond length as in cation **1a** (1.405 Å). The data show that the  $\Delta E_{\pi}$  values in **1b'–e'** are between 6 and 9 kcal/mol smaller than in **1b–e** which were calculated without geometry constraints. Note that the overall weaker attractive interactions in **1b'–e'** are largely compensated by weaker Pauli repulsion so that the net interaction energy  $\Delta E_{\text{int}}$  becomes only 2–3 kcal/mol weaker than in **1b–e**.

Thus, it is clear that the ability of  $\sigma$  C–E bonds to stabilize carbocations in  $\beta$ -position through hyperconjugation increases in the order C–C  $\ll$  C–Si < C–Ge < C–Sn < C–Pb. Our results are in agreement with previous findings by Lambert et al.<sup>11,12,14</sup> and they provide further support for the ability of the EDA method to directly estimate the relative contributions of  $\pi$  interactions which come from hyperconjugation.<sup>5f,5g</sup>

Since the strength of hyperconjugation is directly reflected in the shortening of the H<sub>2</sub>C–C bond lengths it is not surprising that there is a good correlation between the latter bond distances and  $\Delta E_{\pi}$ . As readily seen from Figure 5a, a linear relationship with a correlation coefficient of 0.990 and standard error of 4.3 between both parameters is obtained. Furthermore, the C–E bond lengths which are also affected by the strength of hyperconjugation exhibit a very good linear relationship between the latter parameters (correlation coefficient of 0.996 and standard error of 2.62, Figure 5b).

**Secondary Carbenium Ions.** The optimized geometries of the secondary carbenium ions [HC{CH(EH<sub>3</sub>)<sub>2</sub>}<sub>2</sub>]<sup>+</sup> (**2a–e**) using C<sub>2v</sub> symmetry are depicted in Figure 6. The calculated HC–C distances decrease from 1.443 Å in **2a** to 1.413 Å in **2e**. This is the same trend as in the primary cations **1a–e** but the absolute values for the bond distances in the latter species are smaller than in the respective secondary cation while the C–E bond lengths in **2a–e** are shorter than in **1a–e**. This finding suggests that the individual contribution of one HC(EH<sub>3</sub>)<sub>2</sub> group to the

**TABLE 2: Results of the Energy Decomposition Analysis for Cations 2a–e at BP86/TZ2P<sup>a</sup>**

$$(\text{H}_3\text{E})_2\text{HC}^{\oplus} \begin{array}{l} \nearrow \text{H} \\ \searrow \text{CH}(\text{EH}_3)_2 \end{array}$$

	frag A					frag B				
	<b>2a</b> , E = C	<b>2b</b> , E = Si	<b>2c</b> , E = Ge	<b>2d</b> , E = Sn	<b>2e</b> , E = Pb	<b>2a</b> , E = C	<b>2b</b> , E = Si	<b>2c</b> , E = Ge	<b>2d</b> , E = Sn	<b>2e</b> , E = Pb
symmetry	C <sub>2v</sub>	C <sub>2v</sub>	C <sub>2v</sub>	C <sub>2v</sub>	C <sub>2v</sub>	C <sub>2v</sub>	C <sub>2v</sub>	C <sub>2v</sub>	C <sub>2v</sub>	C <sub>2v</sub>
$\Delta E_{\text{int}}$	−140.4	−145.0	−145.8	−145.1	−143.5	−330.0	−362.5	−372.8	−385.6	−393.8
$\Delta E_{\text{Pauli}}$	322.2	326.4	335.2	348.0	361.5	560.7	565.6	573.4	586.9	605.3
$\Delta E_{\text{elstat}}^b$	−190.4	−182.5	−187.1	−193.5	−199.0	−344.9	−319.3	−326.2	−335.4	−345.2
	(41.1%)	(38.7%)	(38.9%)	(39.2%)	(39.4%)	(38.7%)	(34.4%)	(34.5%)	(34.5%)	(34.6%)
$\Delta E_{\text{Orb}}^b$	−272.3	−288.9	−293.9	−299.6	−306.0	−546.1	−608.7	−620.0	−637.2	−653.9
	(58.9%)	(61.3%)	(61.1%)	(60.8%)	(60.6%)	(61.3%)	(65.6%)	(65.5%)	(65.5%)	(65.4%)
$\Delta E_{\sigma}^c$	−238.1	−242.0	−245.6	−249.2	−254.1	−456.6	−472.8	−475.4	−481.9	−487.5
	(87.4%)	(83.8%)	(83.5%)	(83.2%)	(83.0%)	(83.6%)	(77.7%)	(76.7%)	(75.6%)	(74.6%)
$\Delta E_{\pi}^c$	−34.2	−46.9	−48.4	−50.4	−51.9	−89.5	−135.9	−144.6	−155.3	−166.4
	(12.6%)	(16.2%)	(16.4%)	(16.8%)	(17.0%)	(16.4%)	(22.3%)	(23.3%)	(24.4%)	(25.4%)
$\Delta \Delta E_{\pi}^d$		−	−46.4	−8.7	−10.7	−11.1				
$\Delta E_{\text{prep}}$	21.0	30.1	29.4	29.9	29.7	24.6	37.2	35.0	34.1	31.6
$\Delta E (= -D_e)$	−119.4	−114.9	−116.4	−115.2	−113.8	−305.7	−325.3	−337.8	−351.5	−362.2
$r(\text{CC})$ (Å)	1.443	1.422	1.420	1.417	1.413					
$q(\text{C})^e$	0.189	0.083	0.052	0.017	−0.006					

<sup>a</sup> Energy values in kcal/mol. <sup>b</sup> The percentages in parentheses give the contribution to the total attractive  $\Delta E_{\text{elstat}} + \Delta E_{\text{orb}}$ . <sup>c</sup> The percentages in parentheses give the contribution to the orbital interactions  $\Delta E_{\text{orb}}$ . <sup>d</sup> Increase of  $\Delta E_{\pi}$  with respect to the preceding molecule. <sup>e</sup> Atomic partial charge at central carbon atom.

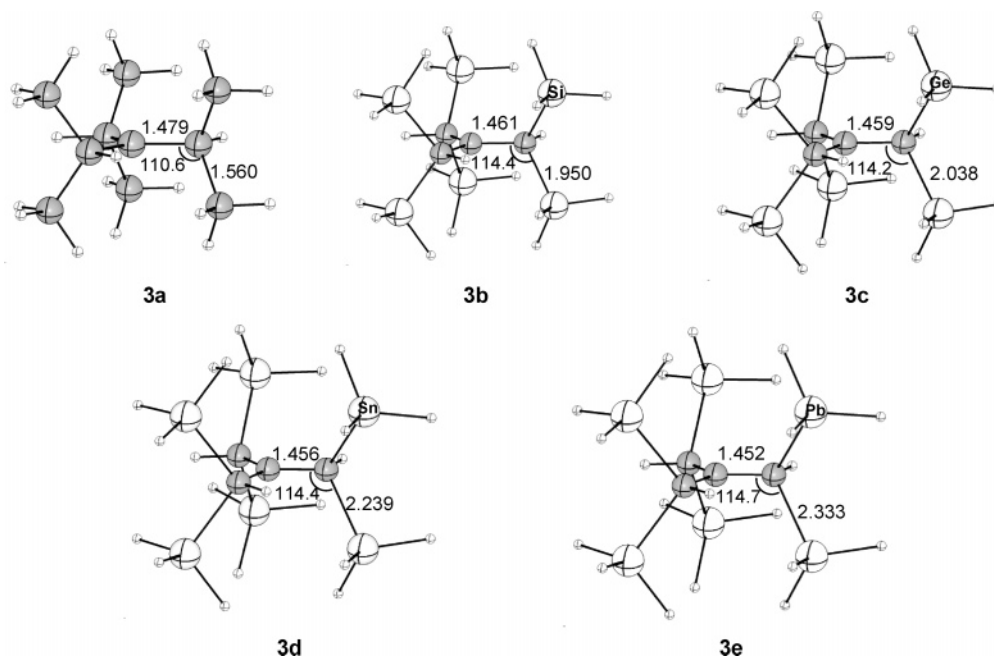


**Figure 7.** Fully optimized geometries at BP86/TZ2P of **3a–e**. Bond distances are given in Å and angles in deg.

hyperconjugation in the secondary cations **2a–e** may be less than the hyperconjugation of the sole HC(EH<sub>3</sub>)<sub>2</sub> group in **1a–e**.

It is interesting compare the calculated geometries of **2b** (E = Si) and **2d** (E = Sn) with the experimental data for the cation [HC{CH(SiMe<sub>3</sub>)(SnMe<sub>3</sub>)<sub>2</sub>}]<sup>+</sup> which were reported by Bochmann et al.<sup>10</sup> The theoretical HC–C distances of model cations **2b** (1.422 Å) and **2d** (1.417 Å) are in excellent agreement with the experimental value of 1.422 Å for the real compound. The theoretical C–SiH<sub>3</sub> distance of **2b** (1.969 Å) also concurs with the experimental C–SiMe<sub>3</sub> distance (1.963 Å) while the calculated C–SnH<sub>3</sub> bond length of **2d** (2.258 Å) is slightly longer than the experimental C–SnMe<sub>3</sub> distance (2.213 Å). The comparison shows that the theoretically predicted geometry should be quite accurate.

Table 2 summarizes the EDA results of carbocations **2a–e**. The calculations were carried out using two fragmentation

schemes. First, we analyzed the interactions between [HC–CH(EH<sub>3</sub>)<sub>2</sub>]<sup>+</sup> and CH(EH<sub>3</sub>)<sub>2</sub> in order to estimate the hyperconjugation of the second substituent in the secondary cations. This scheme is denoted as Frag A in Table 2. In the other partitioning scheme (denoted as Frag B), we analyzed the interactions between two CH(EH<sub>3</sub>)<sub>2</sub> groups and a CH<sup>+</sup> cation in order to estimate the total strength of the hyperconjugation.

The EDA data in Table 2 indicate that the strength of the hyperconjugation of the C–E bonds in the secondary carbenium ions exhibits as expected the same trend as in the primary cations C–C ≪ C–Si < C–Ge < C–Sn < C–Pb. The stronger hyperconjugation of the C–Sn bonds than that of the C–Si bonds which is predicted by the EDA is in agreement with the conclusion of Bochmann et al.<sup>10</sup> that Sn is significantly better in stabilizing the carbocationic center than Si. The absolute values of ΔE<sub>π</sub> for the hyperconjugation of two substituents (frag B) in **2a–e** is clearly larger than the hyperconjugation of one

**TABLE 3: Results of the Energy Decomposition Analysis for Cations 3a–e at BP86/TZ2P<sup>a</sup>**

$$(\text{H}_3\text{E})_2\text{HC}^{\oplus} \begin{array}{l} \diagup \text{CH}(\text{EH}_3)_2 \\ \diagdown \text{CH}(\text{EH}_3)_2 \end{array}$$

	frag A					frag B				
	<b>3a</b> , E = C	<b>3b</b> , E = Si	<b>3c</b> , E = Ge	<b>3d</b> , E = Sn	<b>3e</b> , E = Pb	<b>3a</b> , E = C	<b>3b</b> , E = Si	<b>3c</b> , E = Ge	<b>3d</b> , E = Sn	<b>3e</b> , E = Pb
symmetry	C <sub>3h</sub>	C <sub>3h</sub>	C <sub>3h</sub>	C <sub>3h</sub>	C <sub>3h</sub>	C <sub>3h</sub>	C <sub>3h</sub>	C <sub>3h</sub>	C <sub>3h</sub>	C <sub>3h</sub>
ΔE <sub>int</sub>	-122.2	-123.6	-123.6	-121.9	-120.4	-526.9	-557.8	-568.4	-580.2	-588.2
ΔE <sub>Pauli</sub>	316.2	320.6	328.0	341.3	352.5	581.4	-580.0	588.3	609.6	634.7
ΔE <sub>elstat</sub> <sup>b</sup>	-190.9	-183.2	-186.8	-192.4	-196.6	-465.6	-419.8	-429.2	-443.0	-458.3
	(43.5%)	(41.2%)	(41.4%)	(41.5%)	(41.6%)	(42.0%)	(36.9%)	(37.1%)	(37.2%)	(37.5%)
ΔE <sub>Orb</sub> <sup>lb</sup>	-247.5	-260.9	-264.8	-270.8	-276.4	-642.7	-718.1	-727.5	-746.8	-764.5
	(56.5%)	(58.8%)	(58.6%)	(58.5%)	(58.4%)	(58.0%)	(63.1%)	(62.9%)	(62.8%)	(62.5%)
ΔE <sub>σ</sub> <sup>c</sup>	-223.4	-228.1	-231.5	-235.9	-240.9	-541.2	-564.0	-564.0	-572.9	-578.7
	(90.3%)	(87.4%)	(87.4%)	(87.2%)	(87.2%)	(84.2%)	(78.5%)	(77.7%)	(76.7%)	(75.7%)
ΔE <sub>π</sub> <sup>c</sup>	-24.1	-32.9	-33.3	-34.9	-35.4	-101.5	-154.1	-162.6	-173.9	-185.8
	(9.7%)	(12.6%)	(12.6%)	(12.8%)	(12.8%)	(15.8%)	(21.5%)	(22.3%)	(23.3%)	(24.3%)
ΔE <sub>prep</sub>	24.3	33.8	32.9	33.7	34.5	35.6	51.1	47.2	45.0	41.9
ΔE(=–D <sub>c</sub> )	-97.9	-89.8	-90.6	-88.2	-85.9	-491.3	-566.7	-521.2	-535.2	-546.3
r(C C) (Å)	1.479	1.461	1.459	1.456	1.452					
q(C) <sup>d</sup>	0.201	0.104	0.073	0.038	0.016					
q(E) <sup>e</sup>	-0.004	0.351	0.323	0.428	0.415					

<sup>a</sup> Energy values in kcal/mol. <sup>b</sup> The percentages in parentheses give the contribution to the total attractive ΔE<sub>elstat</sub> + ΔE<sub>orb</sub>. <sup>c</sup> The percentages in parentheses give the contribution to the orbital interactions ΔE<sub>orb</sub>. <sup>d</sup> Atomic partial charge at central carbon atom. <sup>e</sup> Atomic partial charge at atom E.

substituent in **1a–e** but the increase is not a factor of 2. The rise in the  $\Delta E_\pi$  values is only between 43.3% for E = C (**1a** to **2a**) and 26.2% for E = Pb (**1e** to **2e**). Thus, the average hyperconjugative stabilization of one CH(EH<sub>3</sub>)<sub>2</sub> group in **2a–e** is weaker than the hyperconjugative stabilization of the same CH(EH<sub>3</sub>)<sub>2</sub> group in **1a–e**. This is in agreement with the calculated C–CH(EH<sub>3</sub>)<sub>2</sub> bond lengths in the primary and secondary cations. The EDA results for the fragments A show that the consecutive influence of the two substituents gives much weaker hyperconjugation for the second CH(EH<sub>3</sub>)<sub>2</sub> group than for the first. Note that the increase in the total hyperconjugative stabilization when one goes from E = C to E = Si is higher for the secondary carbenium ions ( $\Delta\Delta E_\pi = 46.4$  kcal/mol, Table 2) than for the primary cations ( $\Delta\Delta E_\pi = 38.0$  kcal/mol, Table 1) but the increase for the heavier group-14 elements Ge–Pb in the series **2a–e** is nearly the same as in **1a–e**. This becomes obvious from Figure 4 which shows the increase of the  $\Delta E_\pi$  values for the two series of compounds. The secondary carbenium ions also show a linear correlation between the strength of hyperconjugation and the C–C bond distance (Figure 5a) and likewise with the C–E bond length (correlation coefficient of 0.990 and standard error of 4.9, Figure 5b).

**Tertiary Carbocations, 3a–e.** Finally, we analyzed the bonding situation in the tertiary carbenium ions **3**. The C<sub>3h</sub> optimized geometries of compounds **3a–e** are depicted in Figure 7. The C–CH(EH<sub>3</sub>)<sub>2</sub> distances are further elongated compared with the respective values for the secondary cations **2a–e**. As with the primary and secondary carbocations, there is a continuous shortening of C–C bonds (from 1.479 Å in **3a** to 1.452 Å in **3e**) but the variation in the interatomic distances is much smaller than in the primary and secondary carbocations. The incorporation of another CH(EH<sub>3</sub>)<sub>2</sub> group also provokes a slight enlargement of the C–C–E angles in compounds **3** compared with cations **1** or **2**.

The EDA results of cations **3** are shown in Table 3. As in the EDA of secondary carbocations, we used two fragmentation schemes. First, we analyzed the interaction of only one CH(EH<sub>3</sub>)<sub>2</sub> group with the cationic center (Frag A in Table 3) using [C(CH(EH<sub>3</sub>)<sub>2</sub>)<sub>2</sub>]<sup>+</sup> and CH(EH<sub>3</sub>)<sub>2</sub> as fragments which were calculated in the electronic doublet state. In the other partitioning scheme (Frag B), we analyzed the interactions between three CH(EH<sub>3</sub>)<sub>2</sub> groups in the doublet state and a C<sup>+</sup> atomic cation calculated in the electronic quartet state. The EDA results reveal the same trends for the tertiary carbocations **3a–e** as for the secondary and primary carbenium ions. The simultaneous hyperconjugative stabilization of three CH(EH<sub>3</sub>)<sub>2</sub> groups is between –101.5 kcal/mol for E = C and –185.8 kcal/mol for E = Pb. The graphical display of the trend of the  $\Delta E_\pi$  values shown in Figure 4 reveals that the hyperconjugative stabilization in **3a–e** has further increased compared with the secondary cations **2a–e** but the rising is smaller than from **1a–e** to **2a–e**. It becomes obvious from both partitioning schemes, that the ability of C–E bonds to stabilize carbocations when placed in the  $\beta$ -position follow the order C  $\ll$  Si < Ge < Sn < Pb. This effect is also reflected in the very good linear relationships between the  $\Delta E_\pi$  values and the C<sup>+</sup>–C bond length (correlation coefficient of 0.999 and standard error of 1.9, Figure 5a) as well as with the C–E bond distances (correlation coefficient of 0.986 and standard error of 6.4, Figure 5b).

## Conclusion

The results of the energy decomposition analysis show that the calculated  $\Delta E_\pi$  values can be used as a quantitative measure to estimate the strength of hyperconjugation in carbenium ions

arising from the interactions of saturated groups possessing  $\pi$  orbitals. The EDA results indicate that the ability of  $\sigma$  C–E bonds to stabilize positive charges by hyperconjugation follows the order C  $\ll$  Si < Ge < Sn < Pb. Hyperconjugation of C–Si bonds is much stronger than hyperconjugation of C–C bonds while the further rising from silicon to lead is smaller and has about the same step size for each element. The strength of the hyperconjugation in primary, secondary and tertiary alkyl carbenium ions does not increase linearly with the number of hyperconjugating groups, the incremental stabilization becomes smaller from primary to secondary to tertiary cations. The effect of hyperconjugation is reflected in the shortening of the C–C bond distances and in the lengthening of the C–E bonds which exhibits a highly linear relationship between the calculated C–C and C–E distances in carbocations **1–3** and the hyperconjugation estimated by the  $\Delta E_\pi$ .

**Acknowledgment.** We are grateful to the Deutsche Forschungsgemeinschaft for financial support of this research. Excellent service by the computer center of the Philipps Universität is gratefully acknowledged. I. Fernández also thanks the Ministerio de Educación y Ciencia (Spain) for a postdoctoral grant.

**Supporting Information Available:** Cartesian coordinates and total energies of all compounds discussed in the text are available free of charge via the Internet at <http://pubs.acs.org>.

## References and Notes

- (1) (a) Olah, G. A., Schleyer, P. v. R., Eds. In *Carbonium Ions*; Wiley-Interscience: New York, 1968–1976; Vols. I–V and references therein. (b) Olah, G. A., Surya Prakash, G. K., Eds. In *Carbocation Chemistry*; Wiley-Interscience: New York 2004.
- (2) Meerwein, H.; van Emster, K.; Joussem, J. *Ber. Dtsch. Chem. Ges.* **1922**, *55*, 2500.
- (3) Birladeanu, L. *J. Chem. Educ.* **2000**, *77*, 858.
- (4) Brown, H. C.; Schleyer, P. v. R. *The Nonclassical Ion Problem*; Plenum Press: New York, 1977.
- (5) (a) Pophristic, V.; Goodman, L. *Nature* **2001**, *411*, 565. (b) Schreiner, P. R. *Angew. Chem., Int. Ed.* **2002**, *41*, 3579. (c) Bickelhaupt, F. M.; Baerends, E. J. *Angew. Chem., Int. Ed.* **2003**, *42*, 4183. (d) Weinhold, F. *Angew. Chem., Int. Ed.* **2003**, *42*, 4188. (e) Mo, Y.; Wu, W.; Song, L.; Lin, M.; Zhang, Q.; Gao, J. *Angew. Chem., Int. Ed.* **2004**, *43*, 1986. (f) Cappel, D.; Tüllmann, S.; Krapp, A.; Frenking, G. *Angew. Chem., Int. Ed.* **2005**, *44*, 3617. (g) Fernández, I.; Frenking, G. *Chem. Eur. J.* **2006**, *12*, 3617. (h) Mo, Y. *Org. Lett.* **2006**, *8*, 535.
- (6) Review: Mo, Y.; Gao, J. *Acc. Chem. Res.* **2007**, *40*, 113.
- (7) Jorgensen, W. L.; Salem, L. *The Organic Chemist's Book of Orbitals*; Academic Press: New York, 1973; p 7.
- (8) (a) Laube, T. *Angew. Chem., Int. Ed. Engl.* **1986**, *25*, 349. (b) Christe, K. O.; Zhang, X.; Bau, R.; Hegge, J.; Olah, G. A.; Prakash, G. K. S.; Sheehy, J. A. *J. Am. Chem. Soc.* **2000**, *122*, 481.
- (9) Hollenstein, S.; Laube, T. *J. Am. Chem. Soc.* **1993**, *115*, 7240.
- (10) Schormann, M.; Garrat, S.; Hughes, D. L.; Green, J. C.; Bochmann, M. *J. Am. Chem. Soc.* **2002**, *124*, 11266.
- (11) Lambert, J. B.; Wang, G.-T.; Teramura, D. H. *J. Org. Chem.* **1988**, *53*, 5422.
- (12) Nguyen, K. A.; Gordon, M. S.; Wang, G.-T.; Lambert, J. B. *Organometallics* **1991**, *10*, 2798.
- (13) Synthetic applications of the  $\beta$ -effect of silicon. (a) Weber, W. P. *Silicon Reagents for Organic Synthesis*; Springer-Verlag: Berlin, 1983. (b) Colvin, E. W. *Silicon Reagents in Organic Synthesis*; Academic Press: London, 1988. (c) Fleming, I. In *Comprehensive Organic Synthesis*; Trost, B. M.; Fleming, I., Paquette, L. A., Eds.; Pergamon Press: Oxford, 1991; Vol. 2, p 563. (d) Fleming, I.; Dunogués, J.; Smithers, R. *Org. React.* **1989**, *37*, 57. Synthetic applications of the  $\beta$ -effect of tin, see (e) Pereyre, M.; Quintard, J.-B.; Rahm, A. *Tin in Organic Synthesis*; Butterworth & Co.: London, 1987. (f) Yamamoto, Y. *Aldrichimica Acta* **1987**, *20*, 45.
- (14) Some pertinent examples: (a) Lambert, J. B. *Tetrahedron* **1990**, *46*, 2677. (b) Lambert, J. B.; Chelius, E. C. *J. Am. Chem. Soc.* **1990**, *112*, 8120. (c) Brook, M. A.; Neuy, A. *J. Org. Chem.* **1990**, *55*, 3609. (d) Yoshida, J.; Maekawa, T.; Murata, T.; Matsunaga, S.; Ise, S. *J. Am. Chem. Soc.* **1990**, *112*, 1962. (e) Siehl, H.-U.; Kaufmann, F.-P.; Apeloig, Y.; Braude, V.; Danovich, D.; Berndt, A.; Stamatis, N. *Angew. Chem., Int. Ed. Engl.* **1991**, *30*, 1479. (f) Hage, G.; Mayr, H. *J. Am. Chem. Soc.* **1991**, *113*,

4954. (g) White, J. M.; Robertson, G. B. *J. Org. Chem.* **1992**, *57*, 4638. (h) Lambert, J. B.; Emblidge, R. W.; Malany, S. *J. Am. Chem. Soc.* **1993**, *115*, 1317. (i) Gabelica, V.; Kresge, A. J. *J. Am. Chem. Soc.* **1996**, *118*, 3838. (j) Chan, V. Y.; Clark, C. I.; Giordano, J.; Green, A. J.; Karalis, A.; White, J. M. *J. Org. Chem.* **1996**, *61*, 5227. (k) Lambert, J. B.; Zhao, Y.; Emblidge, R. W.; Salvador, L. A.; Liu, X.; So, J.-H.; Chelius, E. C. *Acc. Chem. Res.* **1999**, *32*, 183. (l) Saguwara, M.; Yoshida, J. *J. Org. Chem.* **2000**, *65*, 3135.
- (15) (a) Bickelhaupt, F. M.; Baerends, E. J. In *Reviews in Computational Chemistry*; Lipkowitz, K. B., Boyd, D. B., Eds.; Wiley-VCH: New York, 2000; Vol. 15, p 1. (b) te Velde, G.; Bickelhaupt, F. M.; Baerends, E. J.; van Gisbergen, S. J. A.; Fonseca Guerra, C.; Snijders, J. G.; Ziegler, T. *J. Comput. Chem.* **2001**, *22*, 931.
- (16) (a) Fernández, I.; Frenking, G. *J. Org. Chem.* **2006**, *71*, 2251. (b) Fernández, I.; Frenking, G. *Chem. Commun.* **2006**, 5030. (c) Fernández, I.; Frenking, G. *Faraday Discuss.* **2007**, *135*, 403.
- (17) Becke, A. D. *Phys. Rev. A* **1988**, *38*, 3098.
- (18) Perdew, J. P. *Phys. Rev. B* **1986**, *33*, 8822.
- (19) Snijders, J. G.; Baerends, E. J.; Vernooijs, P. *At. Data Nucl. Data Tables* **1982**, *26*, 483.
- (20) Krijn, J.; Baerends, E. J. *Fit Functions in the HFS-Method*; Internal Report (in Dutch); Vrije Universiteit: Amsterdam, The Netherlands, 1984.
- (21) (a) Chang, C.; Pelissier, M.; Durand, Ph. *Phys. Scr.* **1986**, *34*, 394. (b) Heully, J.-L.; Lindgren, I.; Lindroth, E.; Lundquist, S.; Martensson-Pendrill, A.-M. *J. Phys. B* **1986**, *19*, 2799. (c) van Lenthe, E.; Baerends, E. J.; Snijders, J. G. *J. Chem. Phys.* **1993**, *99*, 4597. (d) van Lenthe, E.; Baerends, E. J.; Snijders, J. G. *J. Chem. Phys.* **1996**, *105*, 6505. (e) van Lenthe, E.; van Leeuwen, R.; Baerends, E. J.; Snijders, J. G. *Int. J. Quantum Chem.* **1996**, *57*, 281.
- (22) Hirshfeld, E. L. *Theor. Chim. Acta* **1977**, *44*, 129.
- (23) Baerends, E. J.; et al. *ADF 2003-01*; Scientific Computing & Modelling NV: Amsterdam, The Netherlands, 2003 (<http://www.scm.com/>).
- (24) Ziegler, T.; Rauk, A. *Theor. Chim. Acta* **1977**, *46*, 1.
- (25) Morokuma, K. *J. Chem. Phys.* **1971**, *55*, 1236.
- (26) (a) Frenking, G.; Wichmann, K.; Fröhlich, N.; Loschen, C.; Lein, M.; Frunzke, J.; Rayón, V. M. *Coord. Chem. Rev.* **2003**, *238–239*, 55. (b) Lein M.; Frenking, G. In *Theory and Applications of Computational Chemistry: The First 40 Years*; Dykstra, C. E., Frenking, G., Kim, K.S., Scuseria G. E., Eds.; Elsevier: Amsterdam, 2005; p 291. (c) Esterhuysen, C.; Frenking, G. *Theor. Chem. Acc.* **2004**, *111*, 81. (d) Kovács, A.; Esterhuysen, C.; Frenking, G. *Chem. Eur. J.* **2005**, *11*, 1813. (e) Krapp, A.; Bickelhaupt, F. M.; Frenking, G. *Chem. Eur. J.* **2006**, *12*, 9196.